Numerical optimization of a RIXS spectrometer using raytracing simulations

2016 J. Phys.: Conf. Ser. 738 012104

(http://iopscience.iop.org/1742-6596/738/1/012104)

Numerical optimization of a RIXS spectrometer using ray-tracing simulations

K Lieutenant[1], T Hofmann[1], C Zendler[3,1], C Schulz[1], E F Aziz[1,2], K Habicht[1]

[1] Helmholtz-Zentrum Berlin, Hahn-Meitner-Platz 1, 14109 Berlin, Germany

[2] Department of Physics, Freie Universität Berlin, Arnimallee 14, 14195 Berlin, Germany

[3] European Spallation Source ERIC, Tunavägen 24, 223 63 Lund, Sweden

E-mail: klaus.lieutenant@helmholtz-berlin.de

Abstract. At Helmholtz-Zentrum Berlin (HZB) the end-station PEAXIS (Photo Electron Analysis and X-ray resonant Inelastic Spectroscopy) combining Angle-dependent X-ray Photoelectron Spectroscopy (AdXPS) and Resonant Inelastic X-ray Scattering (RIXS) is currently built. The latter method uses a spherical variable line space (VLS) grating to focus the beam onto the detector. Working in first-order diffraction allows resolving photon energy by transferring the energy-dependent signal to a position-dependent focal spot on the detector. Focusing requires a precise combination of various parameters of the VLS grating and the geometry of the RIXS spectrometer. The VLS grating was optimized by calculating the geometry parameters for different photon energies, simulating the instrument and evaluating the pattern on the detector. As figure of merit we chose the intensity times the square of the resolving power averaged over the photon energies.

1. Introduction

Resonant Inelastic X-ray Scattering (RIXS) is a rapidly evolving technique to study inelastic processes using X-ray synchrotron beams. Due to the wide range of applications [1], spectrometers of this type have recently been built [2] or are under construction at most synchrotrons. At the BESSY II synchrotron, operated by the Helmholtz-Zentrum Berlin (HZB), the PEAXIS end-station offering RIXS measurements [3] is currently under construction. It combines Angle-dependent X-ray Photo-electron Spectroscopy (AdXPS) and RIXS measurements, both for solid and liquid samples, in a energy range of 200 – 1200 eV. The set-up allows measurements in a wide range of momentum transfer by varying the angle of detection between 30° and 150° relative to the incoming X-ray beam.

To perform the AdXPS measurements, a commercial photoelectron analyzer is part of the instrument. The RIXS spectrometer is designed by HZB and has to be optimized thoroughly. The basic idea is to use a grating with a high line density (> 1000 lines/mm) in first-order diffraction. For grazing incidence ($87° < \alpha < 90°$, cf. figure 1), soft X-rays are reflected on the surface of the grating and scattered to a direction that depends on the photon wavelength. This transfers the energy dependent intensity distribution to a position dependent distribution on the detector surface and thus allows precise determination of the photon energy. To achieve a high energy resolution, good optical

focusing from the sample to the detector surface is crucial. This is realized by state-of-the-art photon optics, a spherical variable line space (VLS) grating. Since its line density varies slightly along the beam, aberration effects can be significantly reduced. This optical system is described in the literature [4 - 6]; the analytical formulae are used here to find the best instrument parameters.

Most applications need a high energy resolution, but are also demanding in terms of intensity, because the processes studied by RIXS measurements have a low cross-section. Increasing the sample – detector distance improves the resolution, but reduces the intensity at the detector. So a good compromise for the instrument length as for other parameters has to be found. We decided to optimize the instrument for the highest value of intensity times the square of the resolving power.

As perfect imaging can only be realized for a single photon energy and aberrations increase with energy difference, two gratings are necessary to cover the large photon energy range. Based on existing knowledge, e.g. [2], instruments of different lengths and line densities were simulated using the program RAY [7] and performance compared. In this way preliminary parameter sets for the two gratings were found and published [3]. However, to find out if the set-ups found were really the best choice, the simulation of the RIXS instrument and its data evaluation was combined with numerical optimization using a swarm algorithm. This algorithm was transferred from the simulation package VITESS 3 [8] and adapted to the requirements for the optimization of a RIXS instrument using RAY.

2. Imaging using a VLS grating

The line density distribution of a variable lines space (VLS) grating can be described by a Taylor series

$$a(w) = a_0 + a_1 w + a_2 w^2 + a_3 w^3 + \ldots \tag{1}$$

Imaging using a spherical concave VLS grating of radius R works perfectly only for a single wavelength λ_0 corresponding to a photon energy E_0. (The index 0 denotes parameters for this wavelength.) It can be described using the light path function F. The focal point is then given by the Fermat condition of vanishing derivatives $\partial F/\partial w=0$ and $\partial F/\partial l=0$ [4] (w, l: directions on the grating surface, l along the lines, w perpendicular to the lines). This leads to a set of equations relating the grating parameters R, a_0, a_1, a_2, etc. with the instrument parameters r_{10}, r_{20}, α_0, β_0 and λ_0. These are [5,6]:

$$a_0 = \frac{1}{k\lambda_0}\left[\sin\alpha_0 - \sin\beta_0\right] \quad \Leftrightarrow \sin\beta_0 = \sin\alpha_0 - k\lambda_0 a_0 \tag{2}$$

$$a_1 = \frac{1}{k\lambda_0}\left[\frac{\cos^2\alpha_0}{r_{10}} + \frac{\cos^2\beta_0}{r_{20}} - \frac{\cos\alpha_0 + \cos\beta_0}{R}\right] \tag{3}$$

$$a_2 = -\frac{3}{k\lambda_0}\frac{1}{2}\left[\frac{\sin\alpha_0}{r_{10}}\left(\frac{\cos^2\alpha_0}{r_{10}} - \frac{\cos\alpha_0}{R}\right) - \frac{\sin\beta_0}{r_{20}}\left(\frac{\cos^2\beta_0}{r_{20}} - \frac{\cos\beta_0}{R}\right)\right] \tag{4}$$

$$a_3 = \frac{4}{k\lambda_0}\frac{1}{8}\left[\begin{array}{l}\frac{4\sin^2\alpha_0}{r_{10}^2}\left(\frac{\cos^2\alpha_0}{r_{10}} - \frac{\cos\alpha_0}{R}\right) - \frac{1}{r_{10}}\left(\frac{\cos^2\alpha_0}{r_{10}} - \frac{\cos\alpha_0}{R}\right)^2 + \frac{1}{R^2}\left(\frac{1}{r_{10}} - \frac{\cos\alpha_0}{R}\right) \\ + \frac{4\sin^2\beta_0}{r_{20}^2}\left(\frac{\cos^2\beta_0}{r_{20}} - \frac{\cos\beta_0}{R}\right) - \frac{1}{r_{20}}\left(\frac{\cos^2\beta_0}{r_{20}} - \frac{\cos\beta_0}{R}\right)^2 + \frac{1}{R^2}\left(\frac{1}{r_{20}} - \frac{\cos\beta_0}{R}\right)\end{array}\right] \tag{5}$$

Equation (2) is the so-called grating equation, equation (3) describes the focal condition and equations (4) and (5) minimize aberrations. An additional equation defines focusing along the detector surface, which is inclined by an angle γ relative to the beam direction ([9], see figure 1).

$$\tan\gamma_0 = -r_{20}\frac{\partial\beta}{\partial r_2} = \frac{\cos\beta_0}{2\sin\beta_0 - r_{20}(\tan\beta_0/R + a_1/a_0)} \tag{6}$$

Additionally, the total length L is the sum of r_1 and r_2. There is one more condition needed to solve the system of equations. This is chosen to have the same contributions from sample size and detector cell size to the line width broadening:

$$r_{10} = \frac{S_1\cos\alpha_0}{S_1\cos\alpha_0 + S_2\cos\beta_0\sin\gamma_0}L_0 \qquad r_{20} = L_0 - r_{10} \tag{7a,b}$$

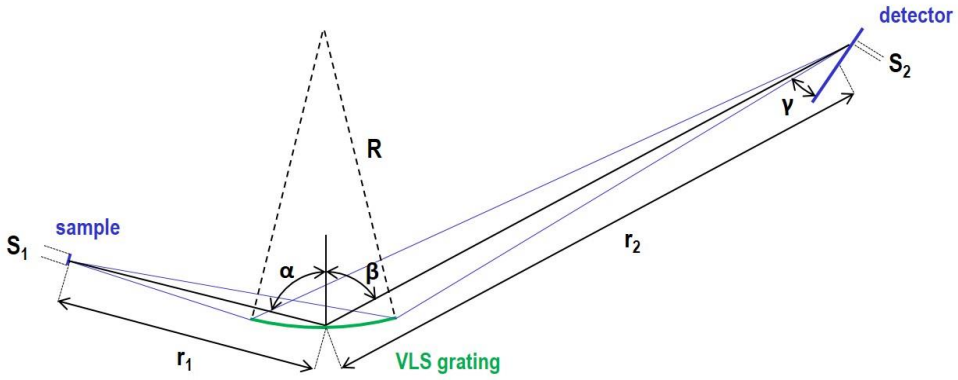

Figure 1. Sketch of the RIXS spectrometer layout showing the relevant instrument parameters

The first-order diffraction is used, i.e. k=1. The illuminated height S_1 of the sample and the (effective) detector cell size S_2 are specific for a certain beamline and instrument (cf. figure 1) and are given as input parameters. The total instrument length L_0, the standard photon energy E_0 and the standard values for incidence angle α_0, detector inclination γ_0 and the line density a_0 at the centre of the grating are now chosen. Equations (2) to (7) allow calculating the instrument parameters β_0, r_{10}, r_{20}, and R. Then the grating parameters a_1 to a_3 can be calculated using equations (3) to (5).

The system is now completely described for the standard photon energy E_0. However to achieve best imaging for photon energies $E \neq E_0$, the parameters α, β, γ, r_1 and r_2 all have to be changed. The equations (2) - (4) and (6) have to be applied again, but now for the parameter set α, β, …r_2. (Equation (5) cannot be fulfilled anymore.) This time the parameters R, a_1, a_2, a_3 are fixed and used to calculate the angles α, β, and γ and distances r_1 and r_2. However, with 4 equations for 5 parameters, there is one free parameter to choose. We choose α – an alternative is γ [10] – equation (2) delivers β then. Knowing α and β allows calculating r_1 and r_2 by combining equations (3) and (4) [3]:

$$r_1 = 1/x_+ \text{ and } r_2 = 1/y_+ \text{ if } x_+>0 \qquad r_1 = 1/x_- \text{ and } r_2 = 1/y_- \text{ if } x_->0 \tag{8}$$

using

$$x_{+,-} = \frac{a_1 hcR + E(\cos\alpha + \cos\beta) - ERy_{+,-}\cos^2\beta}{ER\cos^2\alpha} \tag{9a}$$

$$y_{+,-} = \frac{2ER(E + a_1 hcR/\cos\beta)\sin\alpha + (E^2R\cos\alpha\sin(\alpha-\beta) \pm \sqrt{W}/\cos\beta)/\cos^2\beta}{2E^2R^2(\sin\alpha\cos\beta - \cos^2\alpha\tan\beta)} \tag{9b}$$

with

$$W = E^2R^2\cos^2\alpha\cos^2\beta(8a_0hcR(B\sin\beta - a_2ER\cos^2\beta\sin\alpha/(3a_0)) + E^2\sin^2(\alpha+\beta))$$
$$B = a_2ER\cos^2\alpha/(3a_0) + a_1(a_1hcR + E(\cos\alpha+\cos\beta))\sin\alpha/(2a_0)$$

γ can then be calculated using equation (6).

3. Simulation and evaluation of a RIXS spectrum

3.1. Simulation of a RIXS spectrum

The spectrum is simulated using the RAY software package [7] in its new variant Ray-UI (version 2.7) containing a graphical user interface. Typically 1.5 Mio X-rays are generated in an area of 20 x 5 μm^2, which is the foreseen spot size of the beam at the sample position. They are directed towards the grating which is usually completely illuminated. Only 3 discrete energies E_m-½ΔE, E_m and E_m+½ΔE are generated which produce 3 lines at the detector that allow calculating the resolving power (see chapter 3.2). ΔE was usually 1 eV.

The grating component of RAY considers practically all physical effects that occur when the X-ray beam hits the grating: the reflectivity of the coating, the position-dependent line density, the profile of the lines and deviations from the ideal shape of the grating (the so-called slope error). Here we assume a so-called blaze grating, whose surface is inclined to have specular reflection into the direction of the first-order diffraction (for the standard energy E_0.) This type of grating has a better performance than others because it delivers higher intensity. However, up to now it can only be produced with a maximal line density of 2400 lines/mm. Rays that are not lost at the grating are propagated to the detector. The data is then stored as counts as a function of the position on the detector I(z).

3.2. Evaluation of the simulated RIXS spectra

The separation Δh_m of the 3 lines is calculated from the centers of mass of the outer peaks: $\Delta h_m = |h_3 - h_1|$. The lines have a Gaussian shape. So the FWHM width δh_m can be determined from first and second moment of the intensity distribution as the average over the 3 lines. (The same formula is also used in cases where there is a significant deviation from a Gaussian shape.) The line broadening (compared to the delta function generated in the source) seen in the simulated spectrum arises from aberration effects, the size of the source and the slope error of the grating. The simulation does not include a broadening due to the effective cell size of the detector. So this contribution has to be added giving the total resolving power

$$R_{tot,m} = \frac{\Delta h_m \cdot E / \Delta E}{\sqrt{\delta h_m^2 + \kappa^2 h_{cell}^2 \sin^2 \gamma}} \tag{10}$$

(κ is the ratio of effective detector cell size and physical cell size h_{cell}. A value of κ=1.5 is assumed.)

The relative intensity I_{rel} is defined as the ratio of the number of photons N_{det} counted in the detector to the number of photons emitted by the sample. In a simulation, photons are sent out only into a limited solid angle Ω_g so that I_{rel} can be calculated from the number N_{src} of photons sent as

$$I_{rel} = \frac{\Omega_g}{4\pi} \frac{N_{\mathrm{det}}}{N_{src}} \tag{11}$$

For small inclination angles γ of the detector, a part of the active area is shadowed by the detector frame, which reduces the detector count rate N_{det}. This effect is not included in the simulation and has to be considered in the data evaluation tool. Now the figure of merit FoM_m for one energy E_m can be calculated and averages over the simulated energies determined, either weighted with energy (13b) or not (13a).

$$FoM_m = I_{rel} R_{tot,m}^2 \tag{12}$$

$$FoM_{av} = \frac{1}{M} \sum_{m'=1}^{M} FoM_{m'} \qquad FoM_{wt} = \sum_{m'=1}^{M} E_{m'} FoM_{m'} \Big/ \sum_{m'=1}^{M} E_{m'} \tag{13a,b}$$

4. Numerical optimization of the RIXS spectrometer

4.1. Determination of grating and instrument parameters for a simulation

First, several parameter sets (L_0, E_0, α_0, γ_0, a_0) were simulated and evaluated. It was confirmed that low values of the detector inclination γ give best resolving power - cf. equation (10) - and thus highest figures of merit. On the other hand, shielding by the frame of the detector does not allow using angles below 17°, and the technical realization also prevents angles above 43.6°. Another limitation concerns the distance r_1: the technical realization requires that it is in the range 650 to 1250 mm.

So the angle of incidence α cannot be chosen arbitrarily. Instead, α is first set to α_0 and the system of equations solved - then it is increased until $\gamma(\alpha)$ equals γ_0. Now it is checked if the corresponding value of r_1 is within the given limits. If it is, this parameter set is used for the simulation; if it is not, α is varied until r_1 and γ are within the limits (see figure 2). This procedure is carried out for each parameter set (L_0, E_0, α_0, γ_0, a_0) and each photon energy E_m. In some cases, there are no values for r_1 and γ within the limits fulfilling the equations. In this case, the figure of merit is set to zero.

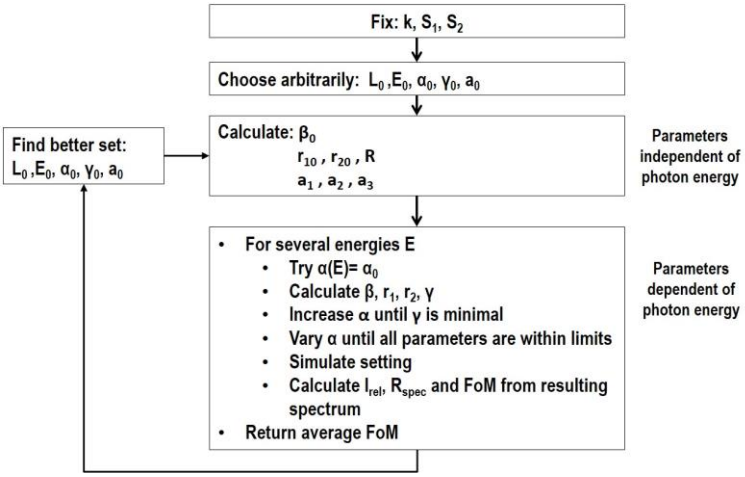

Figure 2. Flow chart of the procedure to find improved settings for the RIXS spectrometer by simulation and data evaluation

4.2. Combination of numerical optimization and simulations

In the new variant Ray-UI of the RAY simulation package [7], the complete instrument is described by an XML file. A simulation can be started by giving this file as a parameter to an executable. This allows running a new simulation by simply substituting the parameter values in the XML file and re-starting the simulation.

To find the best configuration, the particle swarm optimization (PSO) [11] is used: a number of individuals (bees) explores the parameter space, but they are influenced in their search by the results of other individuals. The implementation of this interaction follows the *time-varying acceleration coefficients* (TVAC) method described in [12]. The number of particles (bees) is set to 15 and the maximal number of steps to 80; after 20 steps without improvement the optimization is stopped. Other parameters determine the interaction of the bees. All these optimization parameters are defined in a parameter file.

Wide ranges were chosen for the allowed values in order to find the true optimum: L_0: 2000 – 6000 mm, E_0: 250 – 550 eV (low energy grating) and 500 – 1100 eV (high energy grating), α_0: 82.0° – 89.6°, γ_0: 20.0° – 43.6°, a_0: 600 – 3600 mm^{-1}. The optimization program defines all parameter sets to be tested. The whole simulation and data evaluation software has to deliver values of the figure of merit for each of the parameter sets. The optimization algorithm interprets this result and calculates

new possible parameter sets to be tested. This is continued until the maximum number of steps or the maximum number of steps without improvement is reached.

5. Results

After strong variation during the first 20 to 30 steps, there is clear convergence of the parameters leading to an early completion of the optimization in some cases. Table 1 summarizes different parameter sets that fulfill the equations (2) to (7) for the standard photon energy E_0 and equations (2) to (4), (6) and (7b) for energies $E \neq E_0$ and yield grating distances r_1 and detector inclinations γ within the technical limits for the whole energy range needed. The upper part shows four settings of the low energy set-up (200 to 600 eV) and the lower part four settings of the high energy set-up (400 to 1200 eV). The first setting of each set-up (Lo-C and Hi-C) shows the best parameter set found without optimization. The other settings are the results of different runs of numerical optimization. In each case, 3 photon energies were simulated and evaluated, 223, 400 and 540 eV for the low energy set-up and 487, 800 and 1116 eV for the high energy set-up. The figure of merit was calculated for each energy according to equations (10) to (13).

The first numerical optimizations (Lo-OCV and Hi-OCV) used the same weight for all 3 energies (equation (13a)). This leads to low standard energies E_0 favoring the low energy end of the given energy range. So the total figure of merit was increased by achieving high performance for low energies while losing performance for high energies. As the aim is to have ideally the same performance over the full range, the following optimization runs were performed with a stronger weighting for the high energies (equation (13b). The resulting E_0 values are now much closer to the center of the range and the figures of merit, calculated according to equation (13b), are the highest of all settings simulated.

Table 1. Standard values of the instrument parameters as found by trial and error (Lo-C and Hi-C) and by different runs of numerical optimization, both for the low- and the high-energy set-up of the RIXS spectrometer. FoM-3 is the weighted average over the 3 energies used in the optimization, FoM-8 is the average over 8 energies. Fixed parameters are in italic.

Run	weight	R	FoM-8	FoM-3	L_0 [mm]	E_0 [eV]	α_0 [deg]	γ_0 [deg]	a_0 [mm^{-1}]	R [mm]
Lo-C	-	-	67.2	73.9	*4084*	*400.0*	*87.200*	*20.000*	*2400*	27157
Lo-OCV	const.	var	67.2	68.8	3985	325.8	87.253	20.000	2365	25422
Lo-OEV	E-dep.	var	68.8	77.3	4205	401.6	87.241	20.000	2747	27227
Lo-OEF	E-dep.	fix	69.2	76.1	*4040*	386.5	87.285	20.000	*2400*	27157
Hi-C	-	-	29.2	31.0	*4110*	*900.0*	*88.000*	*20.000*	*2400*	41513
Hi-OCV	const.	var	33.1	29.9	4174	571.4	87.813	20.000	2551	35278
Hi-OEV	E-dep.	var	35.2	36.3	4133	723.9	87.694	20.162	3357	33317
Hi-OEF	E-dep.	fix	34.3	34.3	*4149*	691.0	88.133	20.000	*2400*	41513

However, while these seem to be the ideal parameters, they could not be used for a practical realization: The first problem is that the maximal line density available for a blaze grating is 2400 lines/mm and the result of the optimization yielded higher values, especially for the high energy set-up. The second problem was that the substrates of the gratings were already ordered with the radii obtained for the best settings found without optimization, i.e. Lo-C and Hi-C.

Therefore, new optimization runs were started, keeping the line density a_0 fixed to 2400 lines/mm and the radius to 27157 and 41513 mm resp. Keeping the radius fixed practically fixes L_0 as well. So

the last optimization had only 3 free parameters: E_0, α_0 and γ_0. However, the performance of the optimized setting was about as good as for the 5 parameter optimization.

The relative intensity, the resolving power and the figure of merit as a function of energy are shown in figure 3 in comparison to the settings found without numerical optimization. The comparison clearly shows a gain in performance, in particular a higher resolving power for the low energy end of each energy range.

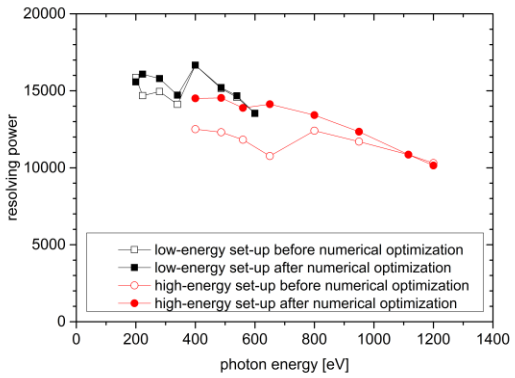

(a)

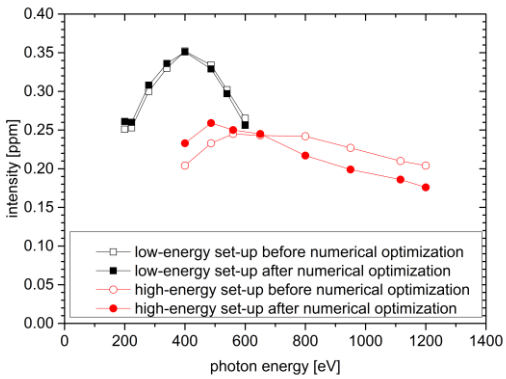

(b)

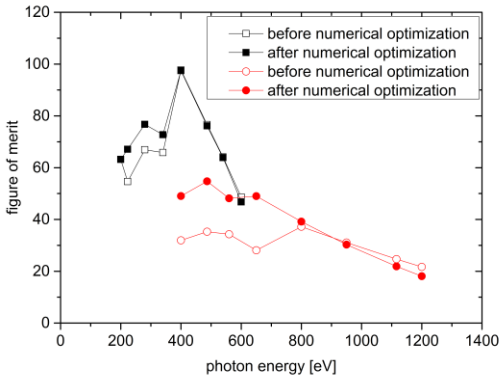

(c)

Figure 3. Comparison of the instrument performance before and after numerical optimization for both, low-energy (black squares) and high energy set-up (red circles): resolving power R (a), detector count rate I_{rel} (b) and figure of merit $FoM=I_{rel} R^2$ (c)

6. Discussion

From several simulations of the RIXS spectrometer [3] a range of the parameter space of good performance was known, but it was not clear if it is the global optimum. So initial values were chosen in a wide range for each parameter to explore the whole parameter space. The result was that all parameter settings of good performance and especially all optimization results were in the known region. However, the performance could be improved significantly, especially for the high energy set-up (see table 1).

The combination of ray-tracing simulations and numerical optimization had been introduced [13] and successfully applied [14] for neutron scattering instruments before. These results show that this combination also works for X-ray instruments. The swarm algorithm is well suited for this kind of optimization, especially if it is not clear where the global optimum is. In this case the swarm algorithm is superior to other algorithms tested in this context [15]; the only drawback is the high number of simulations needed.

The restriction to 3 energies during optimization seems justified: the figures of merit using the average of 3 energies are not very different from that for 8 energies (cf. table 1). It also appeared that using 15 bees was sufficient. On the other hand, a higher number of rays would have been useful, because the figure of merit for one parameter set varied from simulation to simulation. Unfortunately, the number of rays was limited in this version of RAY-UI and the simulation is rather slow. When these weaknesses are overcome in upcoming versions, RAY-UI will be a well suited program to combine with optimization, because the description of the instrument in an XML file makes this combination very easy.

Interestingly, about the same performance could be achieved with a reduced number of free parameters (cf. optimizations –OEV and –OEF in table 1). For the low energy grating the fixed parameters are quite close to the results of the other optimization; so it is not that surprising that the same figure of merit could be reached. But for the high energy grating, radius and line density were significantly different, while nearly the same figure of merit could be reached (see table 1). This means that there is not a single optimum giving a performance better than all others. Instead there seem to be many optima with comparable figures of merit.

It is important to mention that the limit for the total instrument length L_0 was never reached in any optimization. Of course a short instrument spoils the resolution, because the broadening caused by most parameters (like source size) decreases with increasing length making a long instrument a high resolution instrument. However the contribution of the slope error is independent of length, which limits the gain in resolving power with increasing length. On the other hand, the count rate is more and more reduced with instrument length. So an intermediate length yields the highest figure of merit. For the slope error of 0.1 arcsec, which could be achieved by our supplier [16], the ideal length L_0 is about 4 m, giving a maximal instrument length of about 4.7 m, which was (fortunately) in the range that can be realized at the foreseen beamline position.

7. References

[1] Simon M and Schmitt T 2014 *J. Electron Spectrosc Relat. Phenom*. **188** 1
[2] Ghiringhelli G et al. 2006 *Rev. Sci. Instrum.* **77** 113108
[3] Lieutenant K, Hofmann T, Schulz C, Yablonskikh M, Habicht K, Aziz E F 2016 (accepted for publication in *J. Electron Spectrosc. Relat. Phenom.*, DOI: 10.1016/j.elspec.2015.08.009)
[4] Namioka T 1959 *J. Opt. Soc. Am.* **49** (1959) 446
[5] Harada T and Kita T 1980 *Applied Optics* **19** 3987
[6] Howells M R 2009 Gratings and Monochromators *X-Ray Data Booklet* (*LBNL/PUB-490 Rev.3*), ed Thompson A C (Berkeley, California: LBNL) chapter 4.3 pp. 4-16–4-26 (http://xdb.lbl.gov/xdb-new.pdf)
[7] Schäfers F 2008 The BESSY raytrace program RAY *Modern Developments in X-ray and neutron Optics* (*Springer Series in Optical Sciences* vol 137) eds Erko A, Idir M, Krist Th and Michette A G (Berlin: Springer-Verlag) chapter 2 pp 9–41
[8] Zendler C, Lieutenant K, Nekrassov D and Fromme M 2014 *J. Phys.: Conf. Ser.* **528** 012036
[9] Osborn K D and Callcott T A 1995 *Rev. Sci. Instrum.* **66** 3131
[10] Strocov V N et al. 2011 *J. Synchrotron Rad.* **18** 134
[11] Kennedy J and Eberhart R 1995 *Proc. IEEE Int. Conf. Neural Networks* **1-6** 1942
[12] Ratnaweera A, Halgamuge S and Watson H C 2004 *IEEE Transactions on Evol. Comp.* **8** 240
[13] Lieutenant K and Zsigmond G 2004 *Physica B* **350** *Suppl. 1* E687
[14] Klenø K H, Lieutenant K, Andersen K and Lefmann K 2012 *Nucl. Instrum. Methods Phys. Res. A* **696** 75
[15] Lieutenant K 2005 *J. Phys.: Cond. Matter* **17** S167
[16] www.zeiss.com